

## Magnetic field penetration depth of polycrystalline (Y,Gd)Ba<sub>2</sub>Cu<sub>3</sub>O<sub>7</sub>, grain-aligned YBa<sub>2</sub>Cu<sub>3</sub>O<sub>7</sub>, and single-crystal Bi<sub>2</sub>Sr<sub>2</sub>CaCu<sub>2</sub>O<sub>8</sub>

Sreeparna Mitra, J. H. Cho, W. C. Lee, D. C. Johnston, and V. G. Kogan

Ames Laboratory—U.S. Department of Energy and Department of Physics, Iowa State University, Ames, Iowa 50011

(Received 17 March 1989)

The magnetic field penetration depths  $\lambda(T)$  of the title compounds are determined from high-field ( $H=2.5$  to 5 T) magnetization  $M$  versus applied magnetic field  $H$  isotherms, by use of a new method of data analysis in the region  $H_{c1} \ll H \ll H_{c2}$  where  $M$  is reversible and linear in the logarithm of  $H$ . All of the  $\lambda(T)$  results are consistent with behavior expected from BCS theory, indicating a nodeless superconducting order parameter. The magnitudes of  $\lambda(0)$  are similar to reported values obtained using independent methods.

The magnetic penetration depth  $\lambda$  of a superconductor governs its magnetic behavior and provides insight into the pairing mechanism. There have been many measurements of both the magnitude and temperature dependence of this quantity for the high- $T_c$  cuprates, but the results are sometimes conflicting. The techniques utilized so far for YBa<sub>2</sub>Cu<sub>3</sub>O<sub>7</sub> (Y-Ba-Cu-O) include muon-spin rotation ( $\mu$ SR),<sup>1,2</sup> ac,<sup>3</sup> and dc (Ref. 4) magnetic susceptibility  $\chi(T)$ , low-field Meissner effect,<sup>5,6</sup> neutron reflection,<sup>7</sup> microwave surface impedance,<sup>8,9</sup> and kinetic inductance<sup>10</sup> measurements. Most of these experiments give results consistent with conventional  $s$ -wave pairing,<sup>1,2,4-6,8,10</sup> while others suggest a different pairing mechanism as reflected in a non-BCS temperature dependence of  $\lambda$ .<sup>3,9</sup>

Most published work with polycrystalline samples does not address the highly anisotropic nature of these materials and at best can give only a rough averaged value of  $\lambda$ . Herein, we present determinations of  $\lambda(T)$  for polycrystalline Y-Ba-Cu-O and GdBa<sub>2</sub>Cu<sub>3</sub>O<sub>7</sub> (Gd-Ba-Cu-O) obtained from high-field magnetization  $M$  versus applied magnetic field  $H$  isotherms in the intermediate-field region  $H_{c1} \ll H \ll H_{c2}$  where  $M(H)$  is (nearly) reversible, using the new analysis technique suggested by Kogan, Fang, and Mitra.<sup>11</sup> Our method allows us to obtain a well-defined average value ( $\bar{\lambda}$ ) of  $\lambda$ , in which the  $\lambda$  anisotropy and the angular distribution of crystallites are explicitly taken into account. We also derive  $\lambda(T)$  for grain-aligned Y-Ba-Cu-O with  $H \perp c$  and for a single crystal of Bi<sub>2</sub>Sr<sub>2</sub>CaCu<sub>2</sub>O<sub>8</sub> (Bi-Sr-Ca-Cu-O) with  $H \parallel c$ .

The theoretical basis and motivation for this work has been discussed in Ref. 11, so only a brief summary is provided here. In the high- $T_c$  cuprates, there exists a broad field domain  $H_{c1} \ll H \ll H_{c2}$  in which, on the one hand, the vortex cores are not overlapped and one can use the London approach and, on the other, the depth  $\bar{\lambda}$  substantially exceeds the intervortex spacing  $L$ , so that the vortex-vortex interaction is proportional to  $\ln(L/\bar{\lambda})$ . The reversible magnetization  $M$  in this domain can be shown to be linear in the logarithm of the applied field (see Ref. 11 and references cited therein). The slopes of the straight lines  $M(\ln H)$  are given by

$$\frac{dM(0)}{d(\ln H)} = \frac{\phi_0}{32\pi^2\lambda_{\min}^2}, \quad \frac{dM(\pi/2)}{d(\ln H)} = \frac{\phi_0}{32\pi^2\lambda_{\min}\lambda_{\max}}, \quad (1)$$

for  $H \parallel c$  and  $H \perp c$ , respectively. Here,  $\phi_0$  is the flux quantum  $hc/2e$ ;  $\lambda_{\min}$  and  $\lambda_{\max}$  are related to  $\bar{\lambda}$  by  $\bar{\lambda} = (\lambda_{\min}^2\lambda_{\max})^{1/3}$  and to the supercarrier effective-mass ratio  $m_3/m_1 = \gamma^2$  by  $\lambda_{\min} = m_1^{1/2}\bar{\lambda} = \gamma^{-1/3}\bar{\lambda}$  and  $\lambda_{\max} = m_3^{1/2}\bar{\lambda} = \gamma^{2/3}\bar{\lambda}$  (the masses are normalized by  $m_1^2 m_3 = 1$ ).<sup>12</sup>

In a field of a few tesla,  $M$  is on the order of a few gauss or less. Therefore, differences between the magnetic induction, the internal field, and the applied field are small both in their values and directions. For this reason, demagnetization effects can be neglected in this field regime, thereby allowing one to obtain the magnetization of a powder sample with randomly oriented grains by direct summation of the magnetic moments of the individual grains. For the powder averaged magnetization  $\bar{M}$  thus obtained from Eqs. (1) we find<sup>11</sup>

$$d\bar{M}/d(\ln H) = (\phi_0/64\pi^2\bar{\lambda}^2)g(\gamma),$$

where

$$g(\gamma) = \gamma^{-1/3}\{\gamma + (\gamma^2 - 1)^{-1/2} \ln[(\gamma^2 - 1)^{1/2} + \gamma]\}. \quad (2)$$

One can find  $\bar{\lambda}$  at various temperatures by measuring the slope of the straight lines  $\bar{M}(\ln H)$ , provided that the anisotropy parameter  $\gamma$  is known and that  $H$  is large enough such that  $\bar{M}$  is (nearly) reversible; the latter condition implies a negligibly small critical current density. Similarly, using grain-aligned powder samples or single crystals, one can determine values of  $\lambda_{\min}(T)$  and  $\lambda_{\max}(T)$  using Eqs. (1). One can then find the anisotropy parameter  $\gamma = \lambda_{\max}/\lambda_{\min} = (m_3/m_1)^{1/2}$ ; for reasons given below, we could not utilize this possibility in the analysis of the present experiments.

The results for three polycrystalline samples are reported here. The first one (Y-Ba-Cu-O 1) was Y-Ba-Cu-O prepared from high-purity Y<sub>2</sub>O<sub>3</sub>, BaCO<sub>3</sub>, and CuO. The mixture was sintered at 940°C for three days with intermediate grindings, then pelletized and sintered in flowing oxygen at 940°C for 20 h and cooled over 36 h to room temperature. A second Y-Ba-Cu-O sample (Y-Ba-Cu-O 2) was prepared and the free-flowing powder was grain aligned below  $T_c$  with  $H \perp c$  *in situ* in the magnetometer as described elsewhere; by comparison with single-crystal results, essentially complete alignment was achieved.<sup>13,14</sup>

The origin of this orientation effect is given in Ref. 15. No reorientation of this Y-Ba-Cu-O 2 sample was detected during the course of our  $M(H)$  experiments with  $H \perp c$ .<sup>16</sup> Both Y-Ba-Cu-O 1 and Y-Ba-Cu-O 2 samples were magnetically pure, showing no impurity Curie ( $C/T$ ) contribution to  $\chi(T)$  above  $T_c$ . Indeed,  $\chi(T)$  increased monotonically with  $T$ ; between  $T_c$  and  $\approx 200$  K, this increase is attributed mainly to superconducting fluctuation diamagnetism.<sup>13</sup> The third polycrystalline sample was pelletized Gd-Ba-Cu-O prepared using the same method as for Y-Ba-Cu-O 1.  $M(H)$  data up to  $H = 5.5$  T were obtained using a Quantum Design superconducting quantum interference device magnetometer. For Y-Ba-Cu-O and Bi-Sr-Ca-Cu-O, the normal state  $M(H, T > T_c)$  was subtracted from the observed values to yield the data, e.g., in Fig. 1 below.

Typical isotherms of  $\bar{M}$  or  $M$  vs  $\ln H$  over a wide temperature range for Y-Ba-Cu-O 1 and Y-Ba-Cu-O 2 are displayed in Figs. 1(a) and 1(b), respectively (similar iso-

therms are obtained for Gd-Ba-Cu-O, after accounting for the magnetism of the  $Gd^{3+}$  ions). For the pressed Y-Ba-Cu-O 1 and Gd-Ba-Cu-O samples, the irreversibility in the data is less than 1% over most of the temperature range. For the oriented powder sample Y-Ba-Cu-O 2, the curves show some irreversibility below about 60 K, with the irreversibility increasing with decreasing temperature. The  $M$  data plotted in Fig. 1(b) are the mean values of data taken with increasing and decreasing field. The largest irreversibility for the set of isotherms shown in Fig. 1(b) was seen at 40 K; these data are shown in the inset. The mean value of the magnetization taken at each field gives rise to a linear  $M(\ln H)$  dependence, as expected (see, e.g., Ref. 17).

The reduced penetration depths  $\lambda(T)/\lambda(0)$  obtained from Fig. 1 using Eqs. (1) and (2) are plotted versus  $(T/T_c)^2$  in Fig. 2(a) for the above polycrystalline samples, along with the predictions for the BCS weak-coupling clean limit and the BCS dirty limit,<sup>18</sup> and the two-fluid relation  $\lambda^2(0)/\lambda^2(T) = 1 - (T/T_c)^4$ .<sup>4</sup> The  $T_c$  values in Fig. 2(a) are taken to be the onset values from Meissner effect measurements in a field of 50 G (cf. Table I and below). The experimental  $\lambda(0)$  values were obtained from extrapolation of the  $\lambda(T)$  data between 45 and 85 K by fitting to the BCS clean-limit result, since in this temperature range the  $M(\ln H)$  curves are straight and reversible in fields between 2.5 and 5 T, whereas at lower temperatures the reversible field region did not ex-

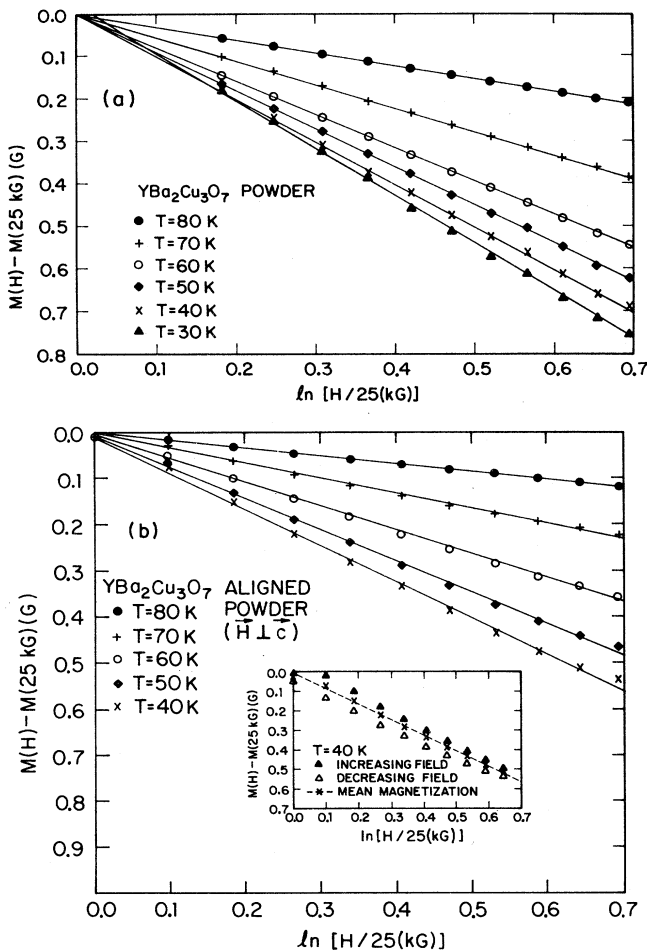


FIG. 1. Typical isotherms of magnetization  $M$  for  $YBa_2Cu_3O_7$  (Y-Ba-Cu-O) plotted against  $\ln(H/2.5$  T). The bottom scale scans magnetic field  $H$  from 2.5 to 5 T. (a) Randomly oriented powder (Y-Ba-Cu-O 1); (b) powder aligned with  $H \perp c$  (Y-Ba-Cu-O 2). The inset shows a typical irreversible  $M(\ln H)$  curve at a low temperature.

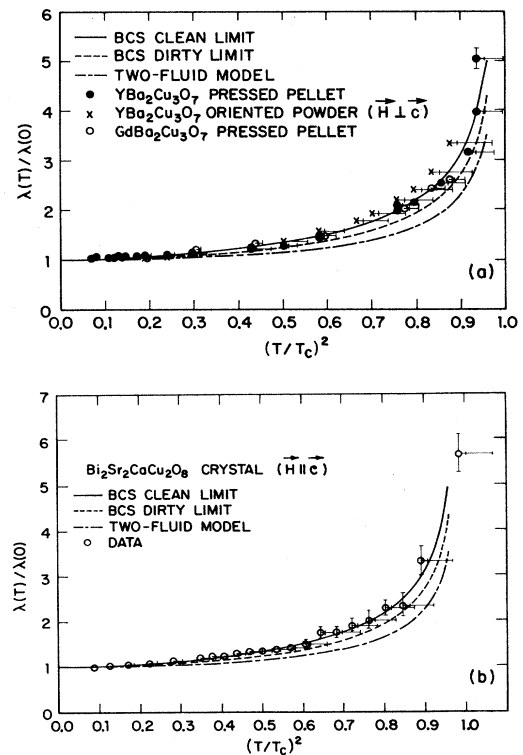


FIG. 2. Penetration depth  $\lambda(T)/\lambda(0)$  vs  $(T/T_c)^2$ . (a) Y-Ba-Cu-O and Gd-Ba-Cu-O polycrystalline samples; (b) Bi-Sr-Ca-Cu-O single crystal.

TABLE I.  $\lambda(0)$  and  $T_c$  values for  $\text{YBa}_2\text{Cu}_3\text{O}_7$  (Y-Ba-Cu-O),  $\text{GdBa}_2\text{Cu}_3\text{O}_7$  (Gd-Ba-Cu-O), and  $\text{Bi}_2\text{Sr}_2\text{CaCu}_2\text{O}_8$  (Bi-Sr-Ca-Cu-O) samples. From Meissner effect data in a field of 50 G,  $T_{c1}$  is the superconducting onset,  $T_{c2}$  is 10% of saturation, and  $T_{c3}$  is the midpoint value. From resistance measurements,  $T_{c1}$  is the onset value,  $T_{c2}$  is the midpoint, and  $T_{c3}$  is the zero-resistance temperature. The  $\bar{\lambda}$ ,  $\lambda_{\min}$ , and  $\lambda_{\max}$  values are extrapolations to  $T=0$ ; for Y-Ba-Cu-O and Gd-Ba-Cu-O,  $\gamma=5$  is assumed.

Sample	$\bar{\lambda}$ (Å)	$\lambda_{\min}$ (Å)	$\lambda_{\max}$ (Å)	$T_{c1}$ (K)	Meissner data			Resistance data		
					$T_{c2}$ (K)	$T_{c3}$ (K)	$T_{c1}'$ (K)	$T_{c2}'$ (K)	$T_{c3}'$ (K)	
Y-Ba-Cu-O 1 <sup>a</sup>	2900	1700	8480	92.1	91.2	89.2	93.5	92.6	91.4	
Y-Ba-Cu-O 2 <sup>b,c</sup>	2200	1290	6430	92.1	91.1	87.5	...	...	...	
Y-Ba-Cu-O 2 <sup>a,c</sup>	...	...	...	91.8	91.4	88.1	92.7	92.0	90.7	
Gd-Ba-Cu-O <sup>a</sup>	2500	1460	7310	92.2	91.4	90.7	92.7	92.0	90.7	
Bi-Sr-Ca-Cu-O <sup>d</sup>	...	3000	...	84.8	84.0	81.3	...	...	...	

<sup>a</sup>Randomly oriented powder pellet.

<sup>b</sup>Free-flowing powder oriented with  $\mathbf{H} \perp \mathbf{c}$ .

<sup>c</sup>Heat-capacity data (Ref. 20) yield the bulk  $T_c \geq 90.8$  K.

<sup>d</sup>Single crystal with  $\mathbf{H} \parallel \mathbf{c}$ .

tend down to 2.5 T. The values of  $\bar{\lambda}(0)$ ,  $\lambda_{\min}(0)$ , and  $\lambda_{\max}(0)$  for the samples are shown in Table I (the latter two were calculated using  $\gamma=5$ ).

A 2.3-mg single crystal of Bi-Sr-Ca-Cu-O was prepared by heating single-phase powder to 950°C and slow cooling to room temperature. The  $\chi(T)$  in  $H=1$  T showed no impurity Curie contribution above  $T_c$ . For  $\mathbf{H} \parallel \mathbf{c}$ ,  $M(\ln H)$  was linear and reversible for  $H=2$  to 5 T above 35 K. The values of  $\lambda_{\min}(T)$  were obtained using the first of Eqs. (1).  $\lambda_{\min}(T)/\lambda_{\min}(0)$  is plotted versus  $(T/T_c)^2$  in Fig. 2(b). The value of  $\lambda_{\min}(0)$  is 3000 Å, about twice that estimated above for Y-Ba-Cu-O. This implies that with  $\mathbf{H} \parallel \mathbf{c}$ ,  $H_{c1}(0)$  for Bi-Sr-Ca-Cu-O is about four times smaller than for Y-Ba-Cu-O.<sup>19</sup> For  $\mathbf{H} \perp \mathbf{c}$ ,  $M$  was small and the signal-to-noise ratio too small to obtain a reliable estimate of  $\lambda_{\max}(0)$ ; further experiments are in progress to determine  $\lambda(T)$  for  $\mathbf{H} \perp \mathbf{c}$  more precisely.

In Fig. 2,  $T_c$  was defined as the superconducting onset as obtained from low-field Meissner data (Table I). With this choice of  $T_c$ ,  $\lambda(T)$  tends to follow the BCS clean-limit prediction, a trend seen by other investigators.<sup>8,10</sup> If the Meissner effect midpoint  $T_c$  values (Table I) are used instead, the  $\lambda(T)$  curves shift towards the two-fluid relation. Horizontal error bars on the data points in Fig. 2 indicate the shift in the data due to this different choice of  $T_c$ ; the lower and upper temperature bars correspond to defining  $T_c$  as the 10 and 50% Meissner transition points, respectively. It is clear from Fig. 2 that the deviation of  $\lambda(T)$  from the results using  $T_c$  as the Meissner effect onset can be substantial (e.g., for Y-Ba-Cu-O 2). Other recent measurements<sup>1,2</sup> also find  $\lambda(T)$  consistent with the two-fluid result if the midpoint  $T_c$  value is used; we have found that if these data are replotted with the onset  $T_c$  used instead,  $\lambda(T)$  is closer to the clean-limit result. We thus reemphasize<sup>5</sup> the importance of the definition of  $T_c$  in interpreting the detailed shape of  $\lambda(T)$ . For sample Y-Ba-Cu-O 2, heat-capacity measurements<sup>20</sup> show a peak at 90.8 K; thus, comparison with Table I suggests that the 10% Meissner transition point may be the best choice for  $T_c$ . Derived  $\lambda(T)$  data which deviate from BCS behavior altogether<sup>3,6</sup> may arise from a broad distribution of  $T_c$  in these samples.

Within the experimental uncertainties, the temperature dependences of  $\lambda$  in Fig. 2 are consistent with the range

predicted from BCS theory. This suggests that there are no nodes in the superconducting order parameter. However, our lowest-temperature data are not sufficiently precise to differentiate between an exponential dependence on temperature (no nodes) and a power-law dependence (nodes present<sup>21</sup>). On the other hand, Gross *et al.*<sup>21</sup> have calculated  $\lambda(T)/\lambda(0)$  for  $T \lesssim T_c$  for the axial (two point nodes) and polar (equatorial line of nodes) states and found that  $[\lambda(T)/\lambda(0) - 1]$  differs considerably from BCS behavior for certain field orientations not only at low temperature for which the power-law behavior is found, but also all the way up to  $T \sim T_c$ . For example, at  $T/T_c=0.75$ , the axial phase has  $\lambda(T)/\lambda(0) \approx 2.0$  for  $H$  perpendicular to the gap symmetry axis, much larger than the BCS value of  $\leq 1.4$  (" $<$ " refers to other than the clean limit). Similarly, for the polar state with  $H$  parallel to the symmetry axis  $\lambda(0.65T_c)/\lambda(0) \approx 1.9$ , whereas the BCS value is  $\leq 1.2$ . These large differences from BCS behavior would have been detected experimentally in the data in Fig. 2 for Y-Ba-Cu-O 2 ( $\mathbf{H} \perp \mathbf{c}$ ) and the Bi-Sr-Ca-Cu-O crystal ( $\mathbf{H} \parallel \mathbf{c}$ ), respectively. Finally, for states with nodes in the gap, the temperature dependences of  $\lambda_{\min}$  and  $\lambda_{\max}$  are, in general, different.<sup>21</sup> In terms of the mass tensor formalism this would imply a temperature-dependent ratio  $m_3/m_1$ , which in turn would lead to a complicated temperature dependence of  $\bar{\lambda}$ , in contrast to the data for the randomly oriented sample Y-Ba-Cu-O 1 in Fig. 2(a). Moreover, that both  $\lambda_{\min}$  for Bi-Sr-Ca-Cu-O in Fig. 2(b) and  $\lambda_{\max}$  for Y-Ba-Cu-O 2 in Fig. 2(a) have the same BCS temperature dependence means that  $\lambda_{\max}(T)/\lambda_{\min}(T) = (m_3/m_1)^{1/2}$  is independent of  $T$  in both materials, provided the underlying mechanism for superconductivity in each is the same. We conclude that our data do not support either the axial or polar state possibilities.

The magnitude of our  $\bar{\lambda}(0)$  for Y-Ba-Cu-O is in good agreement with results of several groups. Jackson *et al.*<sup>4</sup> estimate  $\bar{\lambda}(0) \approx 3000$  Å from dc  $\chi(T)$  measurements. With anisotropy effects taken into account, Schenck<sup>1</sup> finds  $\bar{\lambda}(0) \approx 3000$  Å from  $\mu\text{SR}$  experiments. Recent single-crystal  $\lambda(T)$  data obtained using low-field dc  $M(T)$  (Ref. 5) and  $\mu\text{SR}$  (Ref. 2) measurements yield  $\lambda_{\min}(0) \approx 1400$  Å. Using Eq. (2) and our  $\lambda(0)$  data, we obtain (Table I)  $\lambda_{\min}(0)$  in the range 1290–1700 Å and  $\lambda_{\max}(0)$  between

6400 and 8500 Å; these values yield  $\bar{\lambda}(0) = 2200\text{--}2900$  Å. Here we have assumed the anisotropy ratio  $\gamma = 5$  in accordance with recent estimates.<sup>22</sup> In view of possible differences in preparation, impurities, grain-boundary effects, and other factors, the agreement is quite good. Also, our results are in agreement with estimates of  $\lambda_{\max}(0)$  from the  $\mu$ SR experiments of Uemura *et al.*<sup>1</sup> on grain-aligned powder (6000 Å) and of Harshman *et al.*<sup>2</sup> on single crystals ( $> 7000$  Å).

In summary, we have derived the temperature-dependent penetration depths of  $\text{YBa}_2\text{Cu}_3\text{O}_7$ ,  $\text{GdBa}_2\text{Cu}_3\text{O}_7$ , and  $\text{Bi}_2\text{Sr}_2\text{CaCu}_2\text{O}_8$  from high-field  $M(H)$  isotherms. We have demonstrated that the method is a simple and vi-

able way to estimate  $\lambda(T)$  with anisotropy effects taken into account. Our results for both  $\mathbf{H}\parallel\mathbf{c}$  and  $\mathbf{H}\perp\mathbf{c}$  are consistent with BCS predictions for  $\lambda(T)$  of  $s$ -wave superconductors, indicating a nodeless superconducting order parameter. Our estimates for  $\lambda(0)$  for Y-Ba-Cu-O are in good agreement with recent measurements on single crystals.

Ames Laboratory is operated for the U.S. Department of Energy by Iowa State University under Contract No. W-7405-Eng-82. This work was supported by the Director for Energy Research, Office of Basic Energy Sciences.

- <sup>1</sup>D. R. Harshman *et al.*, Phys. Rev. B **36**, 2386 (1987); Y. J. Uemura *et al.*, *ibid.* **38**, 909 (1988); J. Phys. (to be published); D. W. Cooke *et al.*, Phys. Rev. B **37**, 9401 (1988); **39**, 2748 (1989); A. Schenck, Physica C **153-155**, 1127 (1988).
- <sup>2</sup>D. R. Harshman *et al.*, Phys. Rev. B **39**, 857 (1989).
- <sup>3</sup>J. R. Cooper *et al.*, Phys. Rev. B **37**, 638 (1988).
- <sup>4</sup>E. M. Jackson *et al.*, Physica C **152**, 125 (1988).
- <sup>5</sup>L. Krusin-Elbaum *et al.*, Phys. Rev. Lett. **62**, 217 (1989).
- <sup>6</sup>P. Monod, B. Dubois, and P. Odier, Physica C **153-155**, 1498 (1988).
- <sup>7</sup>R. Felici *et al.*, Nature (London) **329**, 523 (1987).
- <sup>8</sup>A. Porch, J. R. Waldram, and L. Cohen, J. Phys. F **18**, 1547 (1988).
- <sup>9</sup>J. P. Carini *et al.*, Phys. Rev. B **37**, 9726 (1988).
- <sup>10</sup>A. T. Fiory, A. F. Hebard, P. M. Mankiewich, and R. E. Howard, Phys. Rev. Lett. **61**, 1419 (1988).
- <sup>11</sup>V. G. Kogan, M. M. Fang, and Sreeparna Mitra, Phys. Rev. B **38**, 11958 (1988).
- <sup>12</sup>There is a misleading trend in the literature to assign the field direction to the  $\lambda$  values. Which component(s) of the  $\lambda$  tensor is (are) relevant, however, depends not only on the field orientation with respect to the crystal axes, but also on the particular geometry and the type of the experiment in which the penetration depth is measured. For example, if  $H < H_{c1}$  and  $\mathbf{H}\perp\mathbf{c}$  axis of a single-crystal slab (see Ref. 5), the screening currents flow in the "easy"  $ab$  plane and the relevant penetra-

- tion depth is  $\lambda_{\min}$ . If the same experiment is done in intermediate fields (with vortices threading the slab), vortex currents flow not only in the easy plane, but partially along the  $c$  direction. To describe the field distribution of this case one needs both  $\lambda_{\min}$  and  $\lambda_{\max}$  [cf. the second of Eqs. (1)].
- <sup>13</sup>W. C. Lee, R. A. Klemm, and D. C. Johnston (unpublished); R. A. Klemm (unpublished).
- <sup>14</sup>W. C. Lee and D. C. Johnston (unpublished).
- <sup>15</sup>V. G. Kogan, Phys. Rev. B **38**, 7049 (1988).
- <sup>16</sup>Field-induced grain realignment to  $\mathbf{c}\perp\mathbf{H}$  occurred at high fields if the powder was initially aligned above  $T_c$  with  $\mathbf{c}\parallel\mathbf{H}$ ; therefore,  $\lambda(T)$  data for  $\mathbf{H}\parallel\mathbf{c}$  could not be obtained for sample Y-Ba-Cu-O 2.
- <sup>17</sup>A. M. Campbell and J. E. Evetts, *Critical Currents in Superconductors* (Taylor and Francis, London, 1972).
- <sup>18</sup>A. A. Abrikosov, L. P. Gorkov, and I. E. Dzyaloshinski, *Methods of Quantum Field Theory in Statistical Physics* (Dover, New York, 1963).
- <sup>19</sup>H. Zhang *et al.*, Solid State Commun. **67**, 1183 (1988).
- <sup>20</sup>W. C. Lee *et al.* (unpublished).
- <sup>21</sup>F. Gross *et al.*, Z. Phys. B **64**, 175 (1986); see also R. A. Klemm *et al.*, *ibid.* **72**, 139 (1988).
- <sup>22</sup>Y. Iye, T. Tamegai, H. Takeya, and H. Takai, in *Superconducting Materials*, edited by S. Nakajima and H. Fukuyama (Publication Office, Jpn. J. Appl. Phys., Tokyo, 1988), p. 46; D. E. Farrell *et al.*, Phys. Rev. Lett. **61**, 2805 (1988).